Chapter 7

Experimental Study of Current-Voltage Characteristics for Fixed and Solar Tracking Photovoltaics Systems

Chukwuemeka Ikedi

Additional information is available at the end of the chapter

http://dx.doi.org/10.5772/intechopen.79710

Abstract

The efficiency of solar electric systems basically depends on the materials used in making the solar cells and regardless of the type of application: fixed or tracking photovoltaics (PV), the quality and quantity of power produced by PV systems depend on both the amount of solar radiation incident on the solar panels as well as the current and voltage characteristics of the load. This present work, which involves field installation of a fixed PV alongside an existing equivalent tracking PV, simultaneously monitored the current and voltage response of both systems to changing solar radiation and ambient temperatures. The comparative results of the study provide a framework for decision-making on the choice of either of the systems and have shown that in the UK, both systems have a relatively slow electrical response to sunrise while the performance of fixed PV systems approximates that of tracking PV systems at noon time.

Keywords: fixed PV, solar tracking PV, voltage-current (I-V) characteristics, maximum power, solar radiation

1. Introduction

Photovoltaics, otherwise called photoelectricity, is a compound word for photo that is light and voltaic that is electric (from Volta the inventor). It is simply the conversion or generation of electricity from light. Jacques Bequerel, a French physicist discovered in the 1890s, that certain materials produce electric current when exposed to light. This phenomenon is called photoelectric effect and forms the basis for the science and technology of photovoltaics.

Photovoltaics (PV) technology has been in existence for more than 50 years now [1] with various innovative applications. For instance, the Swiss solar aircraft, "Solar Impulse 2", achieved the longest non-stop solo flight in history making the first solar-powered aerial circumnavigation in 2015. The wide range of fixed PV applications include—lighting (e.g. for buildings, streets, traffic signals and navigation), transportation (e.g. solar-powered vehicles, boats, ships), telecommunications, astronomy and space electrical power supplies.

Other applications include roadside emergency telephones, parking ticket machines, remote sensing and cathodic protection of oil and brewery pipe lines.

This chapter presents an overview of basic photovoltaics materials and components and most significantly, investigates and analyses the electrical characteristics of two types of installed PV systems namely: fixed and solar tracking PV simultaneously, under varying solar radiation and temperature conditions in the UK.

By deducing and comparing the maximum power for each of the systems at different points in time, interesting observations were made which led to vital conclusions regarding the relative choice of either of the systems with respect to their respective maximum power performances and cost under similar applications and conditions.

2. Photovoltaic materials and solar panels

In order to appreciate any solar electric or PV system and applications, whether experimental as in this present study or otherwise, a brief overview of the background becomes inevitable.

The basic component of a PV module or panel is the solar cell. Although recent research and innovations have identified some other materials, extensive literature reviews in this study has identified silicon as the key material used in making the solar cells for most PV panels and unless broken or exposed to harmful elements, they could last for a period of more than 20 years and usually protected behind transparent glass materials. Three major configurations of silicon photovoltaic materials were identified in use for solar panels, namely: monocrystalline, polycrystalline and amorphous cells.

Monocrystalline cells: These were found to be the first commercially developed solar cells. They are cut from single crystals of silicon and have an efficiency of about 11–16%. They are chemically stable [2]. They have negligible defects and impurities and are usually grown from a sophisticated but expensive process, known as Czochralski process.

Polycrystalline cells: Cut from many silicon crystals, they have a single colour tone, multiple patterns and an efficiency of about 9–13%. They are cheaper in production than monocrystalline types, but less efficient, because of their light-generated charge recombination effect [3].

Amorphous cells: These are silicon cells in non-crystalline form, usually used in thin film technology. They are cheaper to produce but have a lower operating efficiency of about 3–6% [2]. They decay over time and are usually used in devices like watches, calculators and toys.

Apart from silicon, other crystalline materials are found to be in use for PV solar cells. One of such materials is the compound semiconductor, gallium arsenide (GaAs). PV cells made

http://dx.doi.org/10.5772/intechopen.79710

from GaAs are more expensive but more efficient than silicon cells. They withstand high temperatures and are therefore used in concentrating PV systems and also for applications that demand very high efficiency, irrespective of cost, like in space operations.

Organic materials are now available for use in solar cells. Most organic photovoltaic cells are made from polymers and compared to silicon solar cells, polymer solar cells are lightweight and cheap to fabricate and have safer environmental impact. The capability to be transparent has made polymer solar cells useful in applications like windows, glass walls and skylight roofing devices. One downside with organic solar cells is that they produce a relatively low level of the efficiency compared to silicon materials [4].

Presently, research is advancing towards the development of more efficient and cheaper materials for generating photo electricity. A new approach, using millimetre-sized polycrystalline silicon spheres on thin sheet aluminium foils have been developed by Texas Instruments, US for PV cells.

It is important to note that each silicon solar cell usually has a voltage output of 0.5 V, and when a collection of such cells are electrically connected for the purpose of meeting certain specified load requirements, it is referred to as a PV module or panel. Furthermore, an electrical combination of two or more PV modules or panels to achieve a specific voltage and current as required by a given load or appliance in a particular application is referred to as PV arrays. The individual modules could be either similar or dissimilar and can be connected either in series or in parallel, unlike the case of cells in the module. The systems installed and used in this experimental study consists of an array of two similar solar PV modules electrically connected in series for either of the applications: fixed and tracking. In general, arrays provide increased power output.

The other components of a PV system include the battery, the charge controller and the inverter and when all connected together becomes referred to as photovoltaics generator.

2.1. Fixed and tracking PV

This experimental study simultaneously monitored a fixed and a tracking PV system. It becomes important therefore to provide a brief explanation of both systems. The Earth moves round the Sun in an elliptical orbit; in a counter clockwise direction on an imaginary line called its axis, tilted with respect to the plane of its orbit at an angle of about 23.4°. Due to this movement of the Earth around the Sun and the consequent effect on solar radiation, some PV systems are designed to track the Sun's movement and hence maximise solar incidence on the modules/arrays by maintaining an optimum orientation between the Sun and the solar panels. Such systems are referred to tracking PV. The complex and usually delicate operations involved in tracking PV systems has meant that most PV applications are of the fixed category resulting in benefits of simplicity, least cost and convenience of operation.

On the other hand, fixed PV systems are defined as such because the solar modules or arrays are permanently fixed at a particular angle towards the Sun, with the aim of maximising solar capture. Fixed systems can be installed either as pole mounted, ground mounted or roof mounted systems.

Pole and ground mounted PV's as in this study are usually installed remote from building envelopes, while other types of PV systems are either installed on structured framework on the roofs of buildings or integrated with the building envelope in such a way that it is referred to as building integrated photovoltaic (BIPV). These involve the integration of the PV modules into parts of the fabric of a building as roof tiles, asphalt shingles, facade materials or shading elements. Used in this way, the integrated PV modules replace conventional building envelope materials thereby benefiting from capital cost reduction and hence improved payback period and life cycle cost.

3. Research methodology

As a preliminary step, an extensive review of previous works was carried out prior to this present study. Most work and research carried out earlier on PV materials were found to be mainly on cell characterisation and development [5–7], etc. Shivakumar et al. carried out a test on interface adhesion strength in multilayered structures; Dauskardt et al. examined the mechanisms of debonding in photovoltaic back sheets; Budiman et al. applied Synchrotron X-ray on c-Si Solar PV cells for micro-diffraction analysis, and these are to mention a few. Few researches conducted on solar tracking PV suggest the average experimental gain of tracking PV systems over the fixed types to be about 25% [8–11].

However, when the use or application of fixed and tracking PV systems is considered at different seasons of the year putting into consideration, obtainable costs of maintenance, a controversy begins to arise which seems to question the credibility of the claimed gain of the tracking PV system over the fixed option. Comparative study on specific aspects of the systems such as power outputs gives a clearer understanding of the respective performances.

Further reviews were carried out on current voltage (I-V) characteristics of photovoltaics materials [12–14]. James et al. showed I-V characteristics with reverse bias slopes to be due to wavelengths of light below semiconductor band gap, while Schottky I-V characteristics were due to wavelengths of light above the semiconductor band gap; Zhang et al. proposed a method to predict I-V curves under different operating conditions, while Ibrahim investigated the response of crystalline silicon (Si) solar cell at different conditions of solar irradiance and showed possible performance defects.

This present study simultaneously monitors and compares the voltage–current response of fixed and solar tracking PV systems under the same varying conditions of solar radiation and ambient temperatures.

3.1. Identification and selection of research case study

As a further preliminary step to achieve a good experimental method, a case study was identified for use in the comparative analyses for the two systems, fixed and tracking PV, respectively. One key requirement for the selection of a case study in this study is that the fixed

http://dx.doi.org/10.5772/intechopen.79710

and tracking PV systems should be installed within the same location and at the closest possible vicinity to each other. This becomes necessary to ensure that the ambient temperatures around the two systems are significantly the same under the same solar insolation. Another key requirement or criteria for the selection of a case study is that the two systems must be of the same system specification and size.

The exact location used for the experimental study is the school of the built environment at the University of Nottingham, UK. The geographical and meteorological details of the location are as follows: Latitude 52.5° North, Longitude, Altitude 48 m and Azimuth 0° (true south).

For the photovoltaic systems, the fixed and the solar tracking PV consist of 2 PV modules tied together in serial connections, respectively. The PV module used for the installations is a BP 275F solar module with a nominal peak power (Pmax) of 75.00 W, maximum power voltage (Vmp) of 17.0 V and maximum power current (Isc) of 4.45 A. The extra features on the tracking system include the solar tracking sensor, made of monocrystalline cells and a 24 inch actuator motor jack for the tracking mechanism. The tracking PV system which was originally used to power a water fountain was already existing while the tracking PV was installed right beside the tracking system for the purpose of the comparative analyses in the study.

3.2. Experimental method

The experimental rig for the study consists of fixed and tracking PV systems, each made up of two BP 275 PV modules with the terminals in each system applied to the electrical circuit in **Figure 1**. The two systems were installed to have the same orientation, south facing at zero azimuths with module inclination of 52°s (which approximates the latitude of the location), having a nominal standard test condition (STC) open-circuit voltage of 21.4 V, short-circuit current of 4.75 A and peak power of 75 W.

STC is an abbreviation for the “standard test condition” by which PV modules are tested and calibrated which is insolation level of 1000 W/m^2, air mass of 1.5 AM and cell temperature of 25°C.

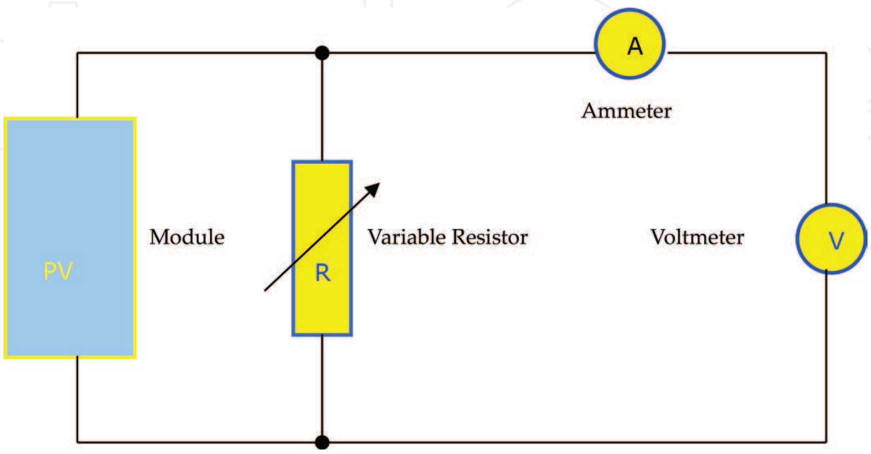

Figure 1. Layout of I-V electrical circuit.

While one of the systems remained fixed relative to the position of the Sun, the other (tracking) kept moving automatically with the aid of a solar tracking sensor and mechanical actuator jack to follow the changing positions of the Sun.

By using a potentiometer type of rheostat, the impedance in the circuitry (**Figure 1**) was varied, while the corresponding current and voltage at each point was monitored and recorded with the aid of the ammeter and the voltmeter.

This process was carried out every 1 h for 2 days between the solar window from 12.00 pm to 4.00 pm for the first day and 9.00–3.00 pm for the second day. One major problem encountered during the measurements was the dramatic change/drop in observed values in some cases due to sudden changes in insolation. This was because UK unlike some tropical locations has a very sloppy insolation gradient within the solar window such that each change in the insolation implies a big difference in the observed values.

4. Results and discussions of experimental work

From the maximum power and the I-V curves, it can be noticed that the gap between the curves for the fixed and tracking systems at each point in time oscillates from infinity towards zero and then towards infinity with noontime as a turning point from sunrise to sunset respectively.

This is because, around and within noontime, the fixed PV system sees the Sun at approximately a perpendicular position and at such point in time also, the tracker device in principle positions the tracking PV system at the same position, hence the difference in performance between the two systems becomes apparently cancelled and so the fixed system almost, approximates to the tracking system.

From noontime towards either sunrise or sunset, the effect of the tracking device on the tracking PV system becomes pronounced as the system becomes more resolved in orientation to the Sun relative to the fixed system.

From basic PV principles [15], the current flowing in the circuit above (**Figure 1**) at each point in time, can be given as

$$I = I_L - I_D(V) \tag{1}$$

assuming a linear superimposition of the photo and dark currents where the photocurrent

$$I_L = eA_C \int_{E_G}^{\infty} S(E)\left[1 - \rho(E, W) - \tau(E, W)\right] dE \tag{2}$$

and the dark current

$$I_D(V) = I_0^{\left[\exp\frac{eV}{(mkT-1)}\right]} \tag{3}$$

where $\alpha(E, W)$ is the spectral absorbance, $S(E)$ is the number of photons of energy E incident on the cell per unit area, A_C is the area of the illuminated cell, k is the Boltzmann's constant, T is the absolute temperature, and m is 1 at high voltages and 2 at low voltages.

From the graphs, (**Figures 2** and **4**), when the resistance is zero, the current in the circuit becomes the maximum (short-circuit current). At this point, the voltage $V = 0$ and from Eq. (1), the short-circuit current becomes

$$I_{SC} = I(V = 0) = I_L \tag{4}$$

Also from the same graphs, at open circuit, the current becomes zero while the voltage becomes the maximum (open-circuit voltage)V_{OC} and expressed as:

$$V_{OC} = \frac{mkT}{q\ln\left\{\frac{I_L}{I_0+1}\right\}} \tag{5}$$

For each of the cases, the area under the curve, which is the product of the voltage and the current, gives a measure of the power output.

At V_{OC} and I_{SC}, the power output becomes zero and maximum at a particular point between these points. This is the point at which the systems deliver the maximum power (maximum power point).

The values of the voltage and current at such points denote the maximum power voltage and the maximum power current V_M and $I_{M,}$ respectively.

The monitored and measured results for the different days are shown and described as follows:

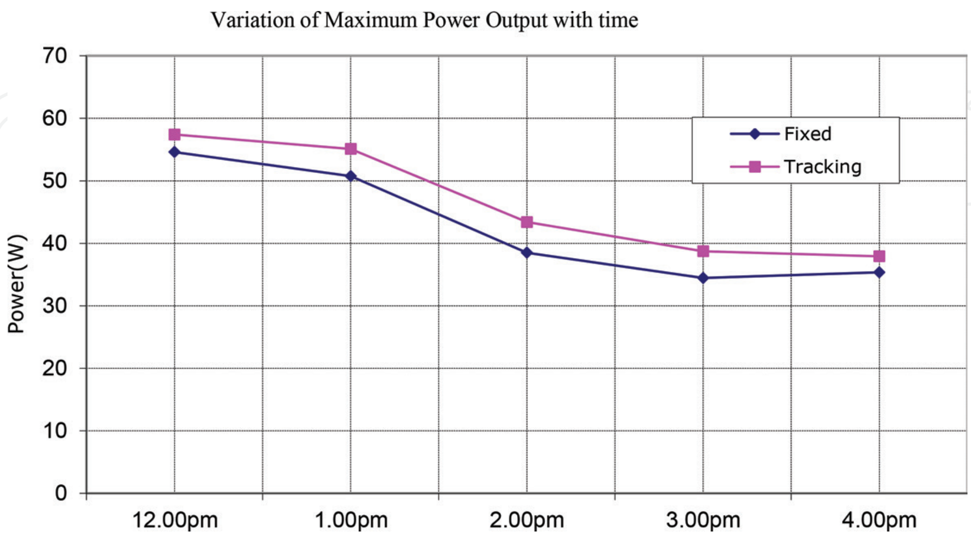

Figure 2. Timely maximum power output.

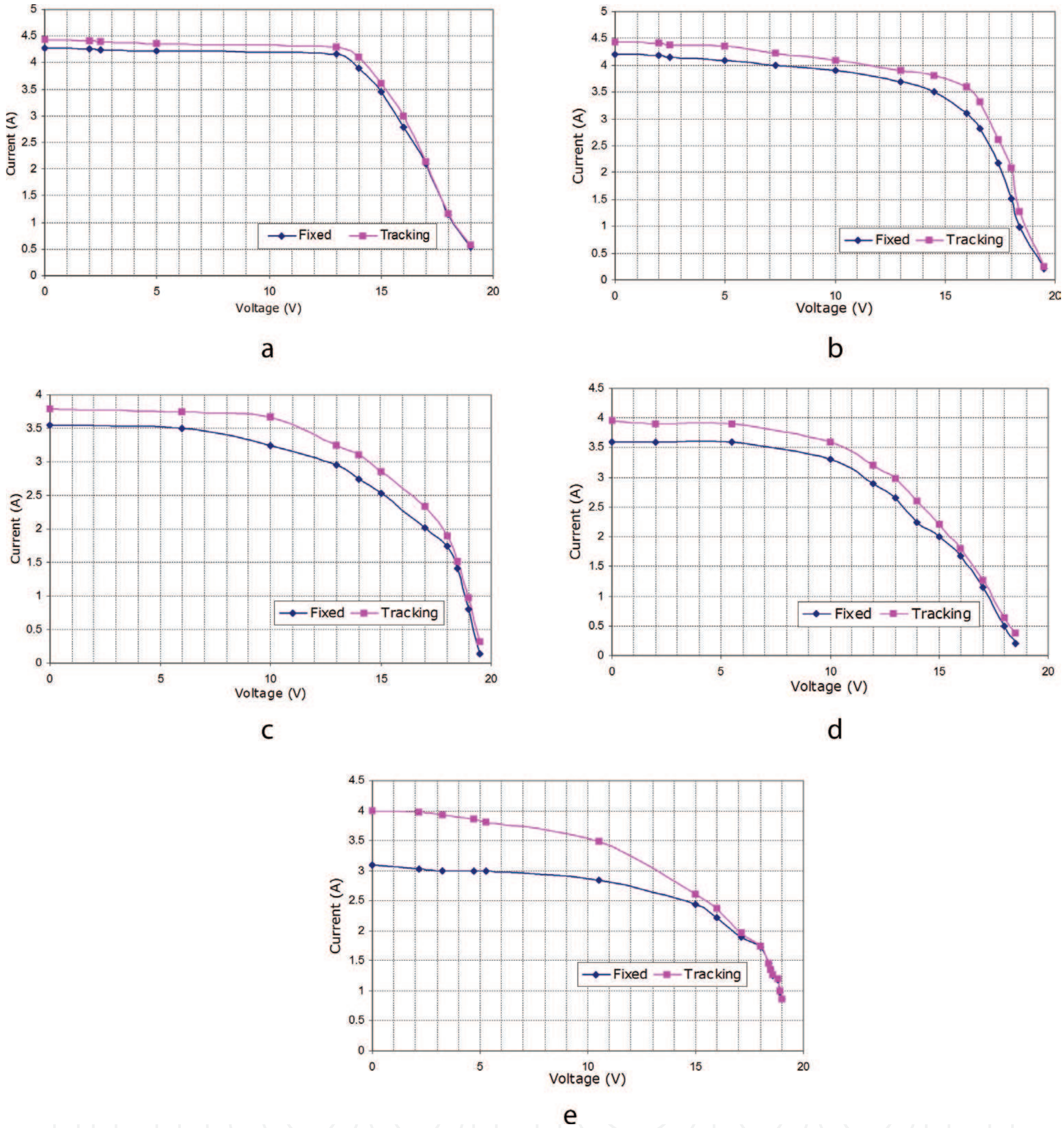

Figure 3. (a) I-V curves at 12.00 pm (hor rad. – 667.9 KWh/m^2. Ambient temp: 22.3°C), (b) I-V curves at 1.00 pm (hor rad. – 517.8 KWh/m^2. Ambient temp: 20.7°C), (c) I-V curves at 2.00 pm (hor rad. 616 KWh/m^2. Ambient temp: 22.7°C), (d) I-V curves at 3.00 pm (hor rad. 517.1 KWh/m^2. Ambient temp: - 21.2°C), (e) I-V curve at 4.00 pm (hor rad. 509.8 KWh/m^2. Ambient temp: 20.8°C).

4.1. Day 1

Table 1 contains the values of the short-circuit current and the open-circuit voltages for each of the observations and summarises the results of the measurements and observations carried out on day 1.

Below is the diagram comparing the maximum power output for the two systems (fixed and the tracking PV) for day 1.

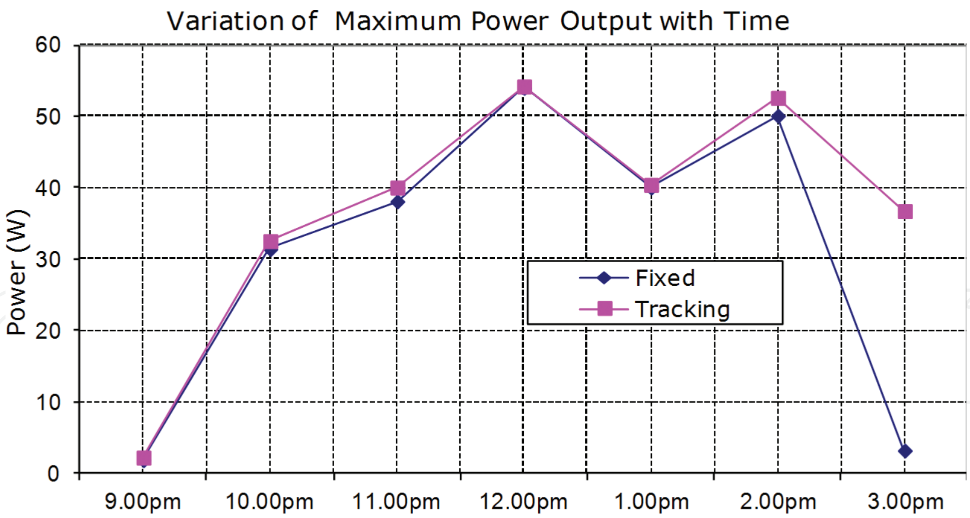

Figure 4. Timely maximum power output for day 2.

Time	Vmp (v)		Imp (A)		Pmp (W)		Voc (V)		Isc (A)	
	Fixed	Trk	Fixed	Trk	Fixed	Trk	Fixed	Trk	Fixed	Trk
12 pm	14.0	14.0	3.90	4.10	54.60	57.40	19.0	19.0	4.28	4.42
1 pm	3.50	3.80	3.70	3.80	50.75	55.10	19.5	19.5	4.20	4.43
2 pm	14.0	14.0	2.75	3.10	38.50	43.40	19.5	19.5	3.54	3.79
3 pm	13.0	13.0	2.65	2.98	34.45	38.74	18.5	18.5	3.60	3.95
4 pm	16.0	16.0	2.21	2.37	35.36	37.92	19.5	19.5	3.09	4.00
Average maximum power (W)					42.73	46.51				
Percentage power gain by tracking (%)						8.85				

Table 1. Measurements and observations for day 1.

It should be recalled from above that power variation approximately oscillates with noontime as the turning point. This is evident from the graphs above as the entire graph for the case of the respective date, represents only about one half of the daily solar window. As earlier pointed out, this was due to the poor climatic condition (Uneven radiation gradient) during the earlier part of the day before noontime.

Nevertheless, the picture of the entire cycle may be observed in the next investigation (**Figure 3**).

It can be concluded from the graphs that the average daily maximum power of the two systems increases from sunrise and peaks around noontime and then gradually decreases towards sunset with the tracking system maintaining a higher output at all times.

The response to sunrise and sunset generally depends on season and climatic conditions of a location [16], for instance, in temperate locations like some parts of Africa, PV panels would be readily responsive to the solar position as at 7.30 am where as in the UK during the time of this experimental work, the graphs of the two systems (fixed and tracking) were almost parallel to the voltage axis as at 9.00 am (**Figure 4a**).

Finally, the voltage-current characteristics was plotted and investigated under varying load conditions (resistance), solar insolation and ambient temperature.

The diagrams below (**Figure 3a–e**) show the I-V curves every 1 h from 12.00 pm to 4.00 pm for day 1.

One interesting thing to note in the above graphs (**Figure 3a–e**) is the change in the power margin between the two systems. Around noontime, the power margin tends very close to zero. The reason for this is explained in the third paragraph of Section 5.

On the other hand, it tends towards infinity around sunrise and sunset. It should also be noticed that at lower load impedance (maximum voltage), the two graphs in most cases begin to overlap.

The explanation for this is that such points approximate to the open-circuit voltage position where the current tends to zero irrespective of fixed or tracking process. Hence, the two graphs overlap.

4.2. Day 2

Table 2 summarises the results of the observations and measurements carried out on day 2. Unlike the previous investigation above, the measurements started 3 h earlier from 9.00 am.

Figure 4 shows the graphical comparison of the observed maximum power output for the fixed and the tracking systems.

It is important to emphasise that the pattern of the maximum power curves (**Figures 2** and **4**) does not take into account the behaviour of the power over the entire interval of the observations and measurements. It depicts the power under the I-V curves with maximum rectangular

Time	Vmp (V)		Imp (A)		Pmp (W)		Voc (V)		Isc (A)	
	Fixed	**Trk**	**Fixed**	**Trk**	**Fixed**	**Trk**	**Fixed**	**Trk**	**Fixed**	**Trk**
9 pm	3.0	3.0	0.6	0.72	1.8	2.16	0.03	0.03	0.63	0.75
10 pm	16.1	16.1	1.95	2.02	31.41	32.54	0.12	0.12	2.8	3.15
11 pm	15.0	15.0	2.54	2.67	38.1	40.05	0.13	0.13	3.27	3.56
12 pm	14.0	16.0	3.86	3.39	54.04	54.24	0.13	0.01	4.09	4.19
1 pm	14.0	16.5	2.86	2.45	40.04	40.43	0.01	0.15	3.57	3.79
2 pm	14.0	14.0	3.58	3.76	50.12	52.64	0.15	0.15	3.95	4.56
3 pm	10.5	10.5	2.87	3.5	3.14	36.75	0.15	0.15	3.0	3.84
Average maximum power (W)					31.24	36.97				
Percentage power gain by tracking (%)						18.34				

Table 2. Measurements and observations for day 2.

http://dx.doi.org/10.5772/intechopen.79710

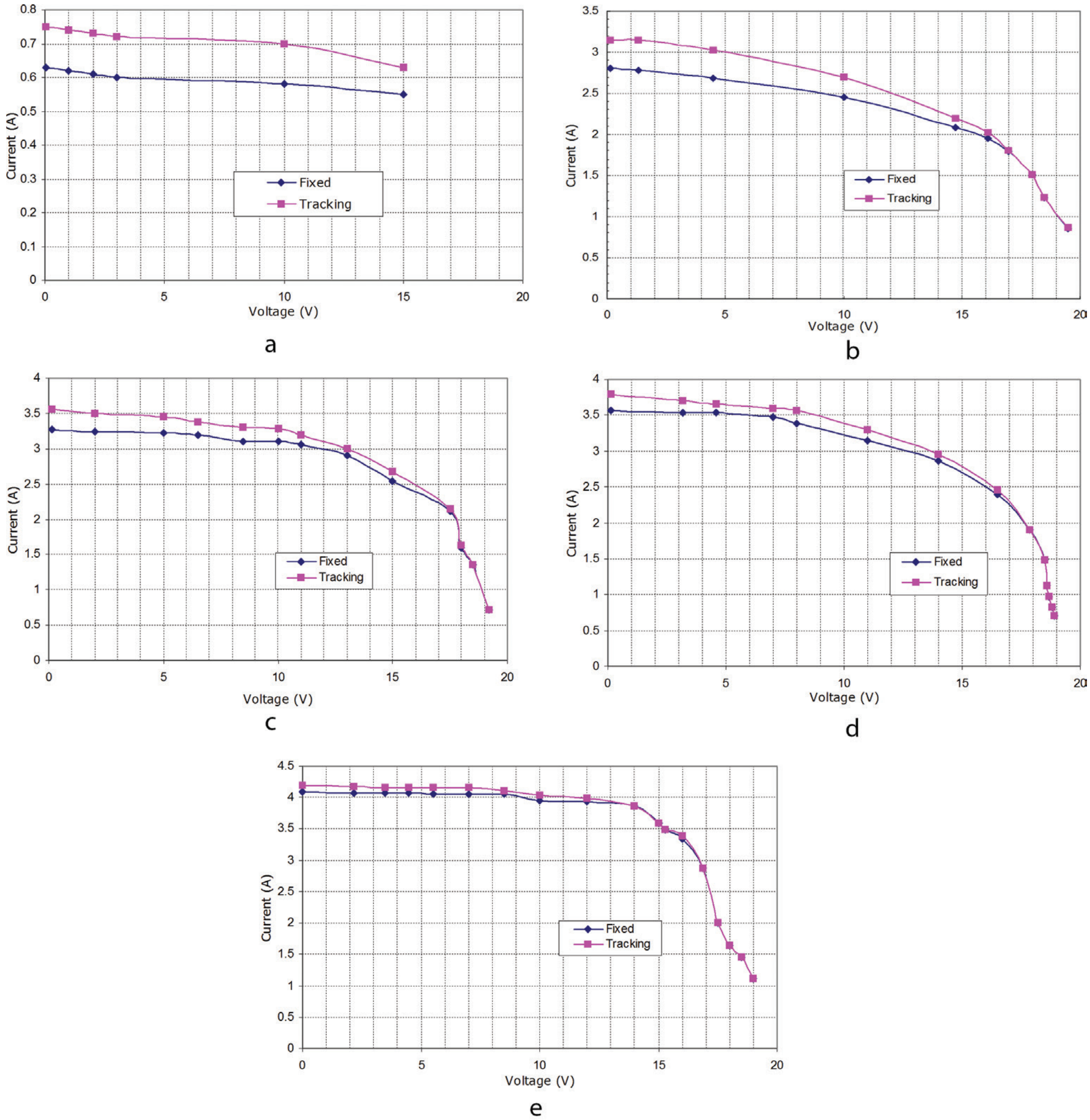

Figure 5. (a) I-V curves at 9.00 am (hor rad. - 223.7 KWh/m². Ambient temp: 14.6°C), (b) I-V curves for 10.00 am (hor rad. – 340 KWh/m². Ambient temp: 16.5°C), (c) I-V curves for 11.00 am (hor rad. - 499.9 KWh/m². Ambient temp: 19.23°C), (d) I-V curves for 12.00 pm (hor rad. – 576.2 KWh/m². Ambient temp: 20.48°C), (e) I-V curves for 1.00 pm (hor rad. – 606.4 KWh/m². Ambient temp: 21.2°C), (f) I-V curves for 2.00 pm (hor rad. – 653.1 KWh/m². Ambient temp: 21.67°C), (g) I-V curves for 3.00 pm (hor rad. – 629.5 KWh/m². Ambient temp: 22°C).

areas. For this reason, the power margin between the fixed and the tracking system at every point along the curves may appear closer as can be seen from the diagram above (**Figure 5**).

The closeness becomes more pronounced in a day with an even high insolation distribution. Comparison of the daily solar radiation for the first and the second day confirm that from the respective diagrams.

Observe the position of the curves in **Figure 5** above at 3.00 pm. At such position, the fixed system was beginning to lose site of sufficient direct radiation as the incident solar angle.

On the other hand, the tracking system was still busy following the Sun at that point as was observed in the field.

The I-V characteristics for day 2 were also plotted and compared for the two systems, fixed and tracking PV. **Figure 5** below show the characteristic curves.

The explanation for the above diagrams is the same with that of **Figure 4(a–e)**. The only notable difference is the appearance of the curves in **Figure 5a** at 9.00 pm.

The reason for this is that at that time for that particular day, the position of the Sun was such that the incidence angle was close to maximum and because the system output has been found to be inversely proportional to the incidence angle, hence the current for both the fixed and the tracking systems at that time appeared parallel to the voltage axis. The values of the current for both systems at the time were approximately the short-circuit currents of 0.63 A and 0.75 A for the fixed and tracking systems, respectively.

Recall that at the short-circuit current, the voltage becomes zero Eq. (4).

Hence, from the relation

$$P = IV \tag{6}$$

The power output for the systems approximated to zero. However, the maximum powers for the systems at that point as can be seen from **Table 2** are 1.8 and 2.16 W, respectively.

5. Conclusions

Key features of the research outcomes which contribute both to the aims of the study and knowledge are outlined below:

1. **Experimental Significance:** The study is absolutely an experimental work which involved a complete PV installation process for the fixed PV alongside the existing tracking PV originally used to power a water fountain. Based on the results of the I-V characteristics for the two systems: fixed and solar tracking PV in UK climate, it can be concluded that in UK and other locations with similar climatic conditions, both the fixed and tracking PV systems have a relatively slow response to sunrise. At noon time in UK, the performance of fixed PV systems approximates that of tracking PV systems. Also in the UK, fixed PV systems compared to tracking PV usually begin to lose sight of sufficient direct radiation after 3.00 pm, while the tracking system relatively remains further active as it still follows the Sun at such points

2. **Decision-Making:** The information gathered from this study can be used to reach decisions on the choice of either of the systems based on the electrical performance of both systems under the same insolation level and ambient temperatures. A common idea prior to this experimental study is that tracking PV generally out-matches the fixed systems. This no doubt is true however, from the results of the I-V characteristics, the margin between the electrical responses of both systems under similar conditions in the UK remain negligible for a longer part of the day. This implies that when the cost and maintenance for

tracking PV systems are put into consideration at such location and other locations with similar climatic conditions, it may make more economic sense to choose the fixed option rather than the tracking PV option.

Finally, it has been shown that the materials used for solar cells in every solar PV module primarily determine the intrinsic efficiency of every solar PV module and system; Gallium arsenide was identified in the study to produce more efficient photovoltaic systems but much more expensive compared to silicon while polymetric or organic materials are much more cheaper but produce less efficient photovoltaic systems. It becomes inevitably necessary therefore to pay more attention to the research and development of cheaper and high efficient solar cell materials.

Author details

Chukwuemeka Ikedi

Address all correspondence to: ikedienergy@yahoo.com

Energy Commission of Nigeria, SunLab Technologies, Nottingham, UK

References

[1] Spanggaard H, Krebs FC. A brief history of the development of organic and polymeric photovoltaics. Solar Energy. 2004;**125**:146-183

[2] Hankins M. Solar Electric Africa. 2nd ed. Common Wealth Science Council; 1995

[3] Halliday D, Resnick R. Fundamentals of Physics. John Wiley and Sons Inc; 2013

[4] Luther J, Nast M, Fisch N, Christoffers D, Pfisterer F, Meissner D, Nitsch J. Solar Technology2008. DOI: 10.1002/14356007.a24_369

[5] Shivakumar R, Tippabhotla SK, Handara VA, Illya G, Tay AO, Novoa F, Dauskardt RH, Budiman AS. Fracture mechanics and testing of interface adhesion strength in multilayered structures. Solar Energy. 2016;**47**:55-89

[6] Dauskardt RH, Novoa D, Fernando C, David M. Environmental mechanisms of debonding in photovoltaic back sheets. Solar Energy. 2014;**87**:93-120

[7] Budiman AS, Illya G, Handara V, Caldwell A, Bonelli C, Kunz M, Tamura N. Enabling thin silicon technologies for next generation c-Si solar PV. Renewable Energy. 2014;**130**:303-308

[8] Bruno R, Bevilacqua P, Longo L, Arcuri N. Small size single-axis PV trackers: Control strategies and system layout for energy optimization. Solar Energy. 2015;**82**:737-743

[9] Bazilian M, Onyeji I, Liebreich M, MacGill I, Chase J, Shah J, Gielen D, Arent D, Landfear D. Re-considering the economics of photovoltaic power. Renewable Energy. 2013;**53**:329-338

[10] Huang BJ, Ding WL, Huang WC. Long-term field test of solar PV power generation using one-axis 3-position sun tracker. Solar Energy. 2011;**85**:1935-1944

[11] Koussa A, Cheknane A, Hadji S, Haddadi M, Noureddine S. Measured and modelled improvement in solar energy yield from flat plate photovoltaic systems utilizing different tracking systems and under a range of environmental conditions. Applied Energy. 2011;**88**:1756-1771

[12] James AR, Kauer M, Mellor AV, Paul N, Nicholas J, Ekins D. Current voltage characteristics of a metallic structure for a hot-carrier photovoltaic cell. PVSC. 2016. DOI: 10.1109/PVSC.2016.7749770

[13] Zhang Y, Gao S, Gu T. Prediction of I-V characteristics for a PV panel by combining single diode model and explicit analytical model. Solar Energy. 2017;**144**:349-355

[14] Ibrahim A. Analysis of electrical characteristics of photovoltaic single crystal silicon solar cells at outdoor measurements. Smart Grid and Renewable Energy. 2011;**2**:4965-4972

[15] Lorenzo E. Solar Electricity: Engineering of Photovoltaics. John Wiley and sons; 2000

[16] Ikedi CU. Numerical assessment of energy contribution by building integrated Photovoltaics in a commercial/office building refurbishment in UK. International Journal for Low Carbon Technologies. 2014;**11**:338-348